RESEARCH ARTICLE

Acteoside inhibits PMA-induced matrix metalloproteinase-9 expression *via* CaMK/ERK- and JNK/NF-κB-dependent signaling

Yong Pil Hwang[1], Hyung Gyun Kim[1], Jae Ho Choi[1], Bong Hwan Park[1], Myung Ho Jeong[2], Tae Cheon Jeong[3] and Hye Gwang Jeong[1]*

[1] Department of Toxicology, College of Pharmacy, Chungnam National University, Daejeon, Republic of Korea
[2] Heart Research Center, Chonnam National University Hospital, Gwangju, Republic of Korea
[3] College of Pharmacy, Yeungnam University, Kyungsan, South Korea

Received: July 21, 2010
Revised: September 16, 2010
Accepted: September 30, 2010

Scope: Acteoside, an active phenylethanoid glycoside found in bitter tea and many medicinal plants, displays chemopreventive properties. The aim of our study was to determine the effect of acteoside on tumor invasion and migration; the possible mechanisms involved in this inhibition were investigated in human fibrosarcoma HT-1080 cells.

Methods and results: We employed invasion, migration and gelatin zymography assays to characterize the effect of acteoside on HT-1080 cells. Transient transfection assays were performed to investigate gene promoter activities, and immunoblot analysis to study its molecular mechanisms of action. We found that acteoside suppresses phorbol-12-myristate-13-acetate (PMA)-enhanced matrix metalloproteinase-9 (MMP-9) expression at the protein, mRNA, and transcriptional levels through the suppression of NF-κB activation. In addition, acteoside repressed the PMA-induced phosphorylation of ERK1/2 (ERK, extracellular regulated kinase) and JNK1/2. Further, we found that acteoside decreased the PMA-induced influx of Ca^{2+} and repressed PMA-induced calmodulin-dependent protein kinase (CaMK) phosphorylation. Furthermore, treatment with BAPTA/AM, W7, or capsazepine markedly decreased PMA-induced MMP-9 secretion and cell migration, as well as ERK and JNK/NF-κB activation.

Conclusion: Acteoside inhibited PMA-induced invasion and migration of human fibrosarcoma cells via Ca^{2+}-dependent CaMK/ERK and JNK/NF-κB-signaling pathways. Acteoside therefore has the potential to be a potent anticancer agent in therapeutic strategies for fibrosarcoma metastasis.

Keywords:
Acteoside / Calcium signaling / Invasion / Matrix metalloproteinase-9 / NF-κB

1 Introduction

There has been increasing interest in natural antioxidants present in fruits, vegetables, herbs, and beverages. Several studies have suggested that intake of food rich in antioxidants is associated with a lower risk of some chronic diseases [1]. Tea is the most popular beverage consumed worldwide. Bitter tea is brewed from the leaves of *Ligustrum purpurascens* which contains acteoside as the major physiologically active component of the plant [2]. Like green tea, bitter tea has also been a popular beverage for a long time in southern China.

Acteoside is a well-studied phenylethanoid glycoside that is widely distributed in the plant kingdom. Acteoside (also called verbascoside) consists of several chemical groups, including caffeic acid, 3,4-dihydroxyphenylethanol, glucose, and rhamnose (Fig. 1A). Several studies have indicated that acteoside exhibits anti-oxidative [3, 4], anti-inflammatory [5], and neuronal protective activities [6]. Recently, it was

Correspondence: Professor Hye Gwang Jeong, Department of Toxicology, College of Pharmacy, Chungnam National University, Daejeon 305-764, Republic of Korea
E-mail: hgjeong@cnu.ac.kr
Fax: +82-42-825-4936

Abbreviations: CaM, calmodulin; **CaMK,** calmodulin-dependent protein kinase; **CPZ,** capsazepine; **ECM,** extracellular matrix; **ERK,** extracellular regulated kinase; **FBS,** fetal bovine serum; **MMP,** matrix metalloproteinase; **MTT,** 3-(4, 5-dimethylthiazol-2-yl)-2, 5-diphenyltetrazoliumbromide; **MT1,** membrane type 1; **PMA,** phorbol-12-myristate-13-acetate; **TIMP,** tissue inhibitors of metalloproteinase; **TRP,** transient receptor potential; **TRPV1,** TRP vanilloid-type 1

*Additional corresponding author: Professor Tae Cheon Jeong
E-mail: taecheon@yumail.ac.kr

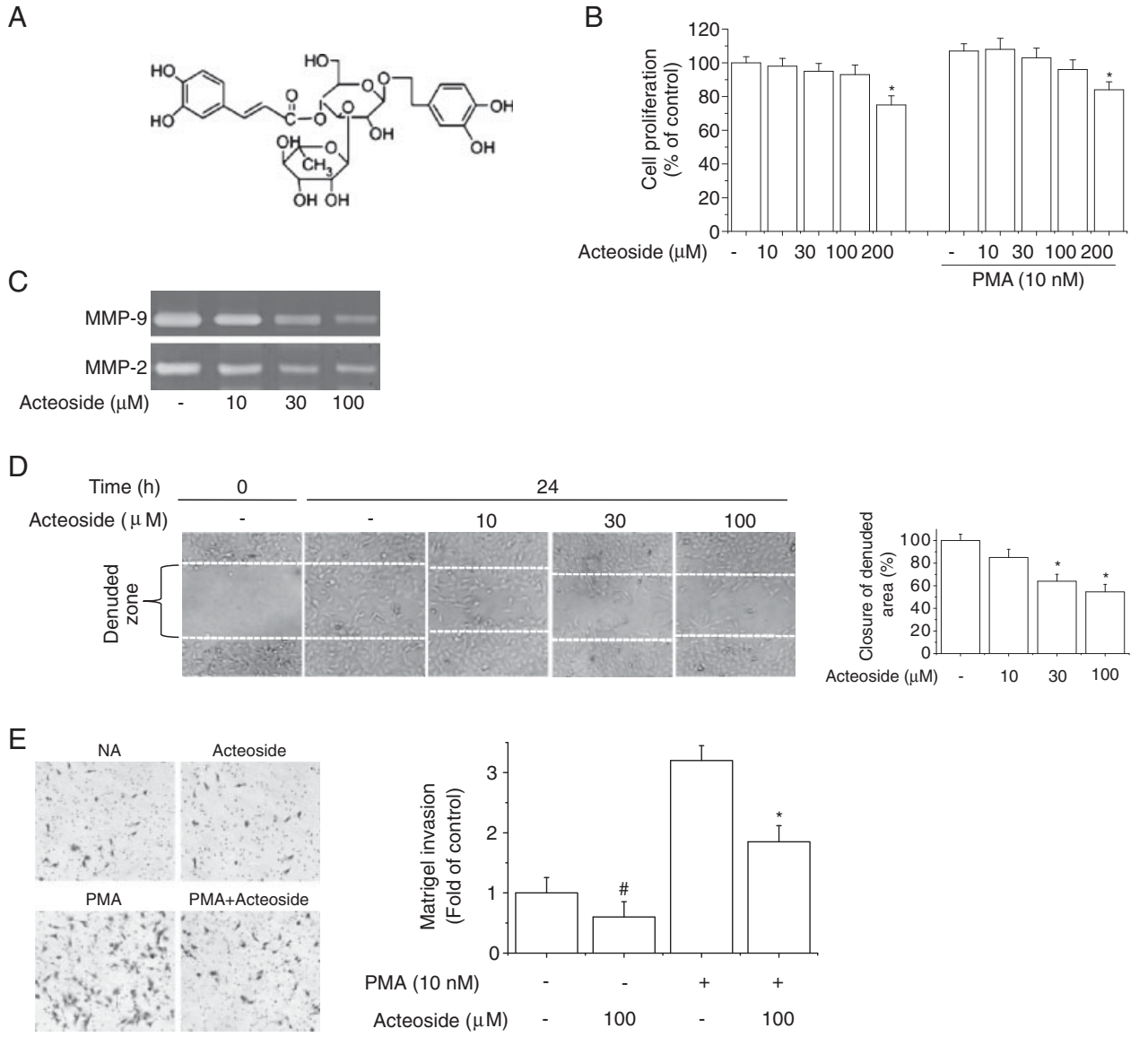

Figure 1. Inhibitory effects of acteoside on the migration and invasion of human fibrosarcoma HT-1080 cells. (A) Structure of acteoside. (B) HT-1080 cells were incubated with varying concentrations of acteoside in the absence or presence of PMA (10 nM) or acteoside for 24 h in serum-free medium, and proliferation was determined by an MTT assay. The data are expressed as the mean ± SD of triplicate experiments. *Significantly different from the control ($p < 0.01$). (C) 80%-confluent HT-1080 cells were treated with various concentrations of acteoside in serum-free medium. The conditioned media were collected after 24 h and gelatin zymography was performed. Each blot is representative of at least three others. (D) Cells were scratched with a pipette tip and treated with acteoside (100 μM) for 24 h. Migrating cells were imaged by phase-contrast microscopy. The data are expressed as the mean ± SD of triplicate experiments. *Significantly different from the control ($p < 0.01$). (E) Cells were pretreated with acteoside (100 μM) or vehicle (0.1% DMSO) followed by PMA treatment (10 nM in 0.1% DMSO) for 24 h. After 24 h, the cells on the bottom of the filter were counted. The data are expressed as the mean ± SD of triplicate experiments. #Significantly different from control ($p < 0.01$). *Significantly different from PMA treatment only ($p < 0.01$).

suggested that acteoside has anti-metastatic [7], anti-proliferative [8], and anti-apoptotic activities [9]. In addition, acteoside inhibited tumor-induced angiogenesis and matrix metalloproteinase (MMP) expression in confrontation cultures of embryoid bodies and tumor spheroids [10].

MMPs play an important role in tumor invasion, angiogenesis, inflammatory tissue destruction, and cancer cell metastasis [11]. These enzymes may contribute to cell invasion-favoring modifications to the matrix, resulting in tumor cell invasion [12]. Invasive cancer cells utilize MMPs to degrade the extracellular matrix (ECM) and basement membrane during metastasis. Among the human MMPs reported to date, MMP-2 and -9, which are expressed abundantly in various malignant tumors, contribute to cancer invasion and metastasis [13]. Generally, MMP-2 is overexpressed constitutively in highly metastatic tumors, whereas

MMP-9 can be stimulated by inflammatory cytokines, epidermal growth factor, or phorbol-12-myristate-13-acetate (PMA) through the activation of various intracellular signaling pathways [11]. Recently, it was suggested that calcium (Ca^{2+}) regulates the expression and activation of MMPs, with particular involvement in the control of MMP-12 activity [14]. Increased extracellular Ca^{2+} levels induce MMP-9 expression in human keratinocytes [15], inhibiting the influx of Ca^{2+} and decreasing the mRNA expression of *MMP-2* [16]. Furthermore, the modulation of intracellular Ca^{2+} levels can alter the secretion of MMP-1 from migrating keratinocytes [17].

Members of the transient receptor potential (TRP) channel superfamily are interesting candidates for the regulation of Ca^{2+} influx and the intracellular Ca^{2+} concentration ($[Ca^{2+}]_i$) in migrating peripheral cells. TRP channels are expressed in almost every cell type, and most are Ca^{2+}-permeable [18]. TRP vanilloid-type 1 (TRPV1) is one of the several nonselective cationic channels, the activation of which induces Ca^{2+} influx; however, this influx can be inhibited by a specific antagonist, capsazepine (CPZ) [19]. Recent data suggest that antagonists of cannabinoid receptors 1 and 2 either alone or in combination with CPZ significantly suppress both cannabidiol-induced tissue inhibitors of metalloproteinase (TIMP)-1 expression and the activation of MAPK p38 and extracellular regulated kinase 1/2 (ERK1/2), thereby suppressing cancer cell invasion [20].

It is accepted that TRPV1 can be phosphorylated by several kinases, including PKA [21], PKC [22], and Ca^{2+}/calmodulin (CaM)-dependent kinase II (CaMKII) [23]. Ca^{2+}/CaM is a Ca^{2+}-binding protein implicated in a variety of cellular functions, including cell growth, proliferation, and migration [24]. Ca^{2+}/CaM itself does not show any catalytic activity, but it regulates the activity of a number of Ca^{2+}/CaM-dependent enzymes, such as CaMK [25] and MAPKs [15]. Previous studies have shown that tumor growth is inhibited by Ca^{2+} channel blockers [26]. Recent evidence has implicated Ca^{2+}/CaM in cancer; abnormal Ca^{2+}/CaM expression is common in certain tumors [27], and specific antagonists of Ca^{2+}/CaM inhibit the growth of a variety of tumor cells [28]. These reports indicate that the inhibition of Ca^{2+} currents could be responsible for the antitumor activity of these drugs. Thus, Ca^{2+}/CaM is a potential target for cancer chemotherapy [29].

Interestingly, recent studies have revealed the ability of acteoside to inhibit the release of β-hexosaminidase and Ca^{2+} influx from IgE-mediated RBL-2H3 cells [30]. Acteoside also inhibited the glutamate-induced influx of Ca^{2+} and displayed significant neuroprotective activity [31]. Although various bioactivity studies of acteoside have been performed, the molecular mechanisms by which the expression of MMP-9 and the invasiveness of HT-1080 cells are regulated *via* acteoside remain unclear. In this study, we examined the effects of acteoside on MMP-9 and -2 expression, and explored the underlying upstream molecular signaling events involved in this regulation.

2 Materials and methods

2.1 Materials

Acteoside was purchased from Chromadex (Santa Ana, CA, USA). BAPTA/AM and *N*-(6-amino-hexyl)-5-chloro-1-naphthalensulfonamide (W7), NF-κB activation inhibitor (JSH-23), PD98059, SB203580, and SP600125 were obtained from Calbiochem (La Jolla, CA, USA). PMA and CPZ were purchased from Sigma Chemicals (St. Louis, MO, USA). 3-(4,5-Dimethylthiazol-2-yl)-2, 5-diphenyltetrazoliumbromide (MTT)-based colorimetric assay kits were purchased from Roche (Indianapolis, IN, USA). RPMI1640, fetal bovine serum (FBS), sodium pyruvate, and Trizol were supplied by Gibco BRL (Grand Island, NY, USA). Antibodies against phospho-MAP kinase, phospho-CaMKs, MMP-2, MMP-9, and NF-κB were purchased from Cell Signaling Technology (Beverly, MA, USA). Antibodies against c-Jun, c-Fos, lamin B, and β-actin were obtained from Santa Cruz Biotechnology (Santa Cruz, CA, USA). The *MMP-9* promoter vector was kindly provided by Dr. W. Eberhardt (Klinikum der Johann Wolfgang Goethe-Universität, Frankfurt/Main, Germany) [32]. The pNF-κB-Luc and pAP-1-Luc reporter plasmids were obtained from Stratagene (La Jolla, CA, USA).

2.2 Cell culture and treatments

HT-1080 cells from the American Type Culture Collection (ATCC, Manassas, VA, USA) were grown in RPMI1640 supplemented with 10% FBS, 100 IU/mL penicillin, and 100 μg/mL streptomycin at 37°C in a 5% CO_2 humidified incubator. Cells were treated with different concentrations of acteoside in the absence or presence of 10 nM PMA for 24 h. Acteoside was dissolved in DMSO (final concentration in culture, 0.1%).

2.3 Measurement of cell proliferation

Cell proliferation was determined by a conventional MTT reduction assay using HT-1080 cells that had been plated at a density of 4×10^4 cells/500 μL in 48-well plates. Following incubation, the cells were treated with MTT solution (final concentration, 1 mg/mL) for 1 h. The dark blue formazan crystals formed in intact cells were solubilized with DMSO, and the absorbance at 570 nm was measured using a microplate reader (Varioskan, Thermo Electron, Berthold, Germany).

2.4 *In vitro* wound-healing assay

HT-1080 cells were seeded into 6-well plates and grown overnight to confluence. The monolayers were then scratched

with a 200-μL pipette tip to create a wound and washed twice with serum-free RPMI1640 to remove floating cells; the medium was then replaced with serum-free medium. The rate of wound closure was assessed and imaged 24 h later. Each value is derived from three randomly selected fields.

2.5 Matrigel invasion assay

HT-1080 cells were incubated in RPMI1640 with 10% FBS and collected by trypsinization. Cells (1×10^5 cells/mL) in serum-free medium were added to the inner cup of a 48-well Transwell chamber (Corning Life Sciences, Oneonta, NY, USA) that had been coated with 50 μL of matrigel (BD Biosciences, Franklin Lakes, NJ, USA; 1:10 dilution in serum-free medium). Medium supplemented with 10% serum or the indicated agent was then added to the outer cup. After 24 h, those cells that had migrated through the matrigel and the 8 μm pore size membrane were fixed, stained, and counted under a light microscope. Each experiment was performed in triplicate.

2.6 RNA preparation, semi-quantitative PCR, and real-time PCR

Total RNA was isolated with an RNA extraction kit (Amersham Pharmacia, Buckinghamshire, UK), and the total RNA concentration was measured spectrophotometrically. RNA (2 μg) was converted to cDNA using an RT-PCR bead kit (Amersham Pharmacia) according to the manufacturer's protocol. *GAPDH* (internal standard) and *MMP-9*, *-2*, *MT1-MMP*, *TIMP-1*, and *TIMP-2* mRNA levels were determined by quantitative real-time RT-PCR as described previously [33, 34].

2.7 Western blot analysis

Following treatment, cells were lysed on ice for 30 min in lysis buffer (120 mM NaCl, 40 mM Tris (pH 8), and 0.1% NP40) and centrifuged at $13\,000 \times g$ for 15 min. The supernatants were then collected and the protein concentrations determined using a BCA protein assay kit (Pierce, Rockford, IL, USA). Lysates (40 μg of protein) were resolved by SDS-PAGE, transferred to a PVDF membrane, and blocked with 1% bovine serum albumin at room temperature for 1 h followed by labeling with primary antibodies for 3 h, and with specific HRP-conjugated secondary antibodies (Santa Cruz Biotechnology) for 1 h. Protein bands were detected using an enhanced chemiluminescence Western blotting detection kit (Pierce).

2.8 Gelatin zymography

The enzymatic activities of MMP-2 and -9 were determined by gelatin zymography. Briefly, cells were seeded, grown to confluence for 24 h, and maintained in serum-free medium. The conditioned media were collected 24 h after stimulation, mixed with nonreducing sample buffer, and subjected to electrophoresis in 10% polyacrylamide gels containing 0.1% w/v gelatin. The gels were then washed with wash buffer containing 2.5% Triton X-100 and 50 mM Tris-HCl (pH 7.5) and incubated at 37°C for 24 h in 50 mM Tris-HCl (pH 7.5), 150 mM NaCl, 5 mM $CaCl_2$, 1 mM $ZnCl_2$, and 40 mM NaN_3. The gel was stained with 0.25% w/v Coomassie brilliant blue in 45% v/v methanol and 1% v/v acetic acid. Gelatinolytic activity was normalized against protein content of the cultured medium as assayed by the BCA kit (Pierce).

2.9 Transient transfection and luciferase assays

To examine promoter activity, we used a dual-luciferase reporter assay system (Promega, Madison, WI, USA). Cells in 48-well plates at 70–80% confluence were incubated with RPMI1640 without serum or antibiotics for 6 h. The cells were then transfected with the *MMP-9* promoter vector AP-1 (5′-TGAC-TAA-3′)$_n$ ($n = 7$) or an NF-κB (5′-GGGGACTTTCC-3′)$_n$ ($n = 5$) reporter vector (1 μg; Stratagene) and pCMV-β-gal (0.5 μg) using Lipofectamine 2000 (Invitrogen, San Diego, CA, USA) according to the manufacturer's protocol. Following incubation, the cells were lysed and luciferase activity was measured using a luminometer (Luminoscan Ascent, Thermo Electron). Luciferase activity was normalized to β-galactosidase activity in the cell lysates and is expressed as the average of three independent experiments. For the analysis of basal NF-κB activity, cells were transiently transfected with Lenti-NF-κB-GFP (System Biosciences, Mountain View, CA, USA) and mixed with Lipofectamine; GFP fluorescence was analyzed by fluorescence microscopy (Axiovert 200M, Carl Zeiss, Jena, Germany).

2.10 Intracellular Ca^{2+} measurement

HT-1080 cells cultured in 24-well plates (2×10^5 cells/mL) in media were loaded with 5 μM Fluo-4-AM (Molecular Probes, Eugene, Oregon), a Ca^{2+}-sensitive dye, for 45 min at 37°C. Following this preincubation, the cells were rinsed three times with media to remove any free dye and incubated for 30 min in medium to allow the de-esterification of all AM esters. The Fluo-4-loaded cells were then stimulated with 100 μM acteoside, 10 nM PMA, 10 μM BAPTA/AM, 40 μM W7, 2 μM CPZ, or the vehicle DMSO. Changes in intracellular Ca^{2+} were measured from fluorescence images obtained at 25 min using an Axiovert 200 M Carl Zeiss Fluorescence microscope (excitation at 385 nm, emission at 512 nm).

2.11 Statistical analysis

All experiments were repeated at least three times. Means ± SD were calculated for each group; Dunnett's *t*-test

was used to calculate statistical significance. Differences were considered statistically significant at $p < 0.01$.

3 Results

3.1 Acteoside inhibits human fibrosarcoma cell invasion and metastasis

Prior to investigating the pharmacological potential of acteoside on PMA-induced MMP activity, we first determined the dose dependence of the cytotoxic effects of acteoside in the absence or presence of PMA (10 nM) for 24 h in HT-1080 cells using the MTT assay. Acteoside at concentrations lower than 100 μM had no cytotoxic effect on the cells and acteoside at 200 μM showed about a 16–25% decrease in cell proliferation in the absence or presence of PMA (Fig. 1B). Thus, acteoside had no significant cytotoxicity in tumor cells at these concentrations (0–100 μM). We next used a gelatin zymography assay to investigate the inhibitory effect of acteoside on MMP-9 and -2 secretion. Treatment with acteoside inhibited the MMP-9 and -2 activity in a dose-dependent manner (Fig. 1C). *In vitro* invasion and migration assays (including Transwell and wound-healing assays) were used to investigate the inhibitory effects of acteoside on the invasive potency of fibrosarcoma HT-1080 cells. As shown in Fig. 1D, HT-1080 cell migration was inhibited by acteoside (Fig. 1D). Similarly, data obtained from matrigel invasion assays demonstrated that PMA-stimulated cell invasion was decreased in the presence of 100 μM acteoside by about 48% (Fig. 1E). Also, treatment with acteoside only inhibited cell invasion by about 40% (Fig. 1E). These results suggest that acteoside prevents the invasion and migration of human fibrosarcoma cells at nontoxic concentrations.

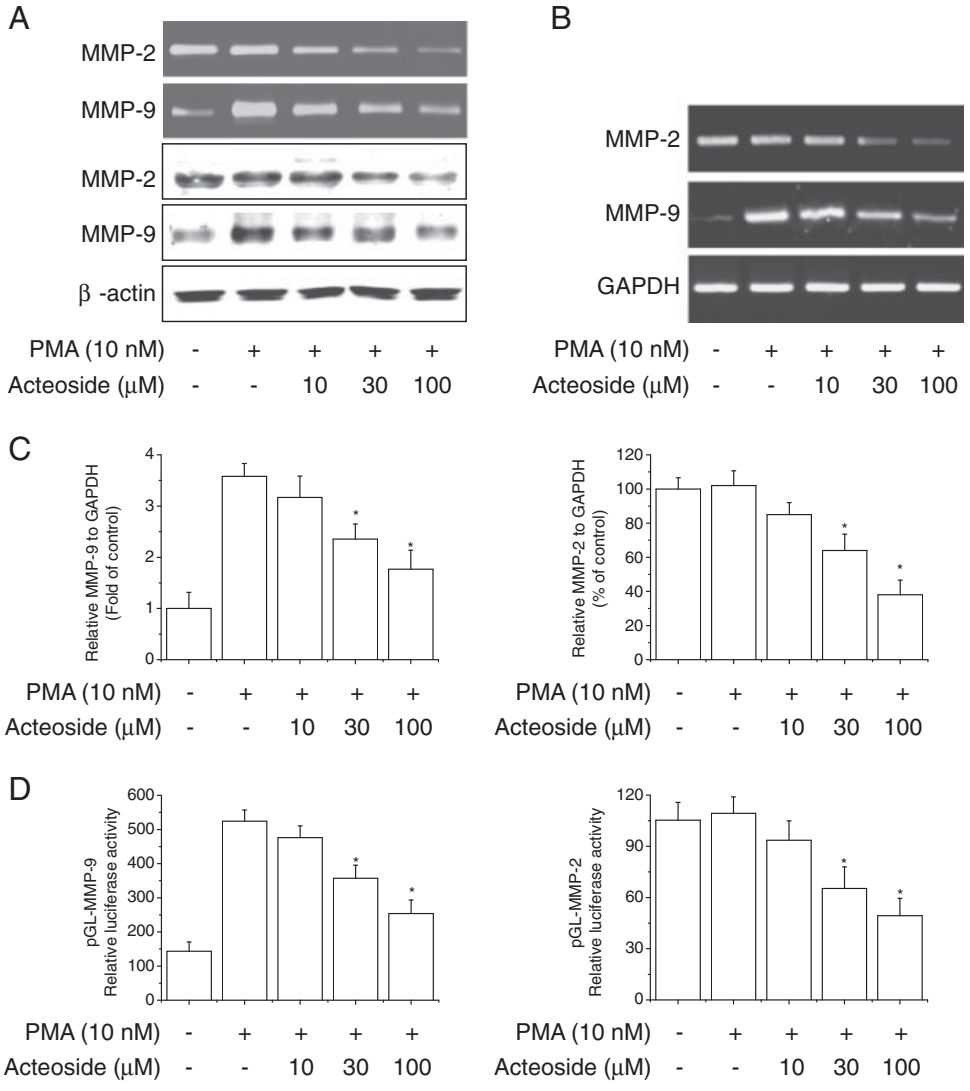

Figure 2. Inhibition of MMP-9 and -2 activity by acteoside. (A) Effects of acteoside on MMP-9 and -2 activity. HT-1080 cells were incubated with varying concentrations of acteoside in the presence of PMA (10 nM) for 24 h. MMP activity in the medium was analyzed by gelatin zymography and Western blotting. (B and C) Effects of acteoside on *MMP-9* and *-2* mRNA expression. HT-1080 cells were incubated with acteoside and/or PMA (10 nM) for 24 h. *MMP-9* and *-2* mRNA expression was analyzed by semi-quantitative RT-PCR or real-time PCR. *GAPDH* was used as an internal control. (D) Effects of acteoside on *MMP-9* and *-2* promoter activity. Cells were transfected with a WT-*MMP-9* or *-2* promoter-containing reporter vector and incubated with various concentrations of acteoside in the absence or presence of PMA (10 nM), as indicated. Luciferase activity was measured 24 h after transfection. *Significantly different from PMA treatment only ($p < 0.01$).

3.2 Acteoside suppresses the expression of MMP-9 and -2

We next examined the effects of acteoside on MMP activity, which is related to the invasion and metastasis of HT-1080 cells. Figure 2A shows that acteoside inhibited PMA-induced MMP-9 activity in a dose-dependent manner, as demonstrated by gelatin zymography and Western blot analysis. Acteoside also inhibited MMP-2 activity in a same manner (Fig. 2A). To determine whether the inhibition of MMP-9 secretion by acteoside was due to decreased transcription, we performed RT-PCR and promoter assays using a luciferase reporter gene linked to the *MMP-9* or *-2* promoter sequence. As shown by semi-quantitative RT-PCR and real-time PCR, the treatment of HT-1080 cells with acteoside decreased the level of PMA-induced *MMP-9* mRNA expression (Fig. 2B and C), indicating that acteoside decreases the transcription of *MMP-9* in response to PMA. In addition, Fig. 2D shows that treatment with acteoside (10–100 μM) decreased PMA-mediated luciferase activity in a dose-dependent manner. Acteoside also inhibited mRNA expression and promoter activity of MMP-2 in a same manner (Fig. 2B–D). No cytotoxicity was observed in the cells exposed to acteoside (data not shown).

3.3 Acteoside suppresses PMA-induced membrane type 1-MMP expression

Membrane type 1 (MT1)-MMP is a key enzyme in tumor metastasis. MT1-MMP activity in pericellular proteolysis directly influences ECM turnover [35]. Moreover, MT1-MMP was identified as the first physiological activator of pro-MMP-2 [12]. Therefore, we sought to determine whether acteoside suppresses MT1-MMP expression in HT-1080 cells stimulated with PMA. Western blot and semi-quantitative RT-PCR analyses revealed that acteoside suppressed PMA-induced MT1-MMP expression at the mRNA (Fig. 3A) and protein levels (Fig. 3B). As MMP activity is tightly regulated by endogenous inhibitors, the TIMPs [36], we further examined the expression of TIMP-1 and -2 by semi-quantitative RT-PCR. Figure 3A shows that the expression level of TIMP-1 and -2 was essentially unchanged by treatment with acteoside, suggesting that acteoside decreases pro-MMP-2 activation through a reduction in MT1-MMP levels.

3.4 Acteoside inhibits the transcriptional activity of MMP-9 through the suppression of PMA-stimulated NF-κB activity

The expression of *MMP-9* is regulated through transcriptional-level interactions between AP-1 and NF-κB and their binding sequences in the *MMP-9* promoter [32]. To investigate whether these transcription factors regulate *MMP-9* in HT-1080 cells, cells were transiently transfected with a reporter gene that included the wild-type *MMP-9* promoter, the NF-κB-responsive promoter, or a promoter with mutations in one or both AP-1 binding sites (Fig. 4A). In cells treated with acteoside in the presence of PMA, the transcriptional activity of the reporter containing NF-κB mutations was unaffected, suggesting that NF-κB is the target of acteoside (Fig. 4A). To

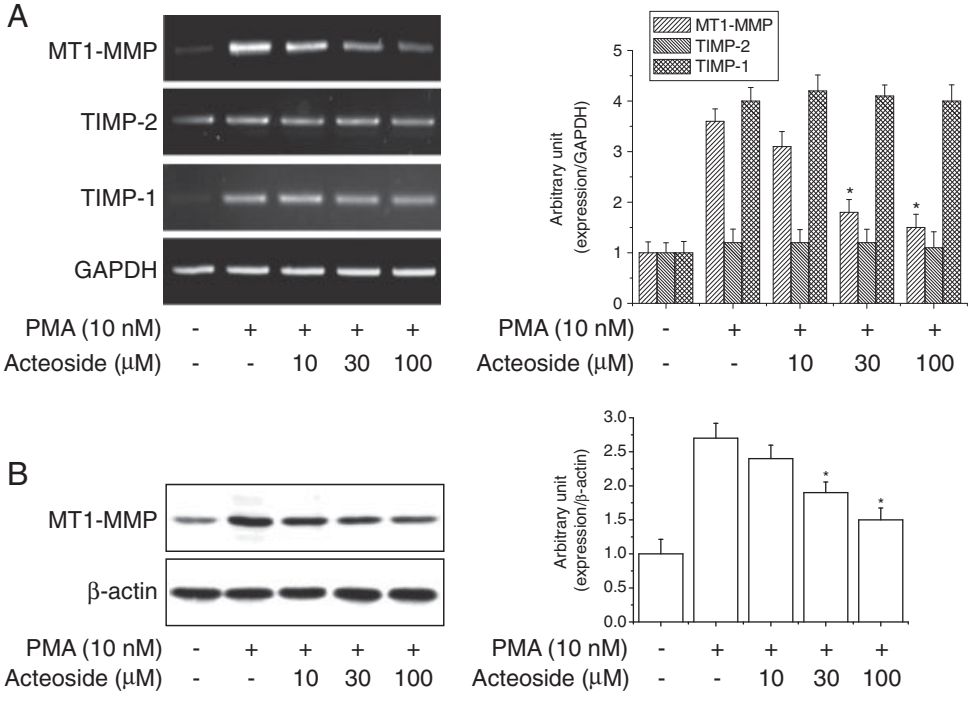

Figure 3. Inhibition of PMA-induced MT1-MMP expression by acteoside. HT-1080 cells were incubated with acteoside and/or 10 nM PMA for 24 h. (A) The mRNA expression of *MT1-MMP*, *TIMP-1*, and *TIMP-2* was analyzed by semi-quantitative RT-PCR. (B) The expression of MT1-MMP was analyzed by Western blotting. GAPDH or β-actin was included as an internal control. *Significantly different from PMA treatment only ($p<0.01$).

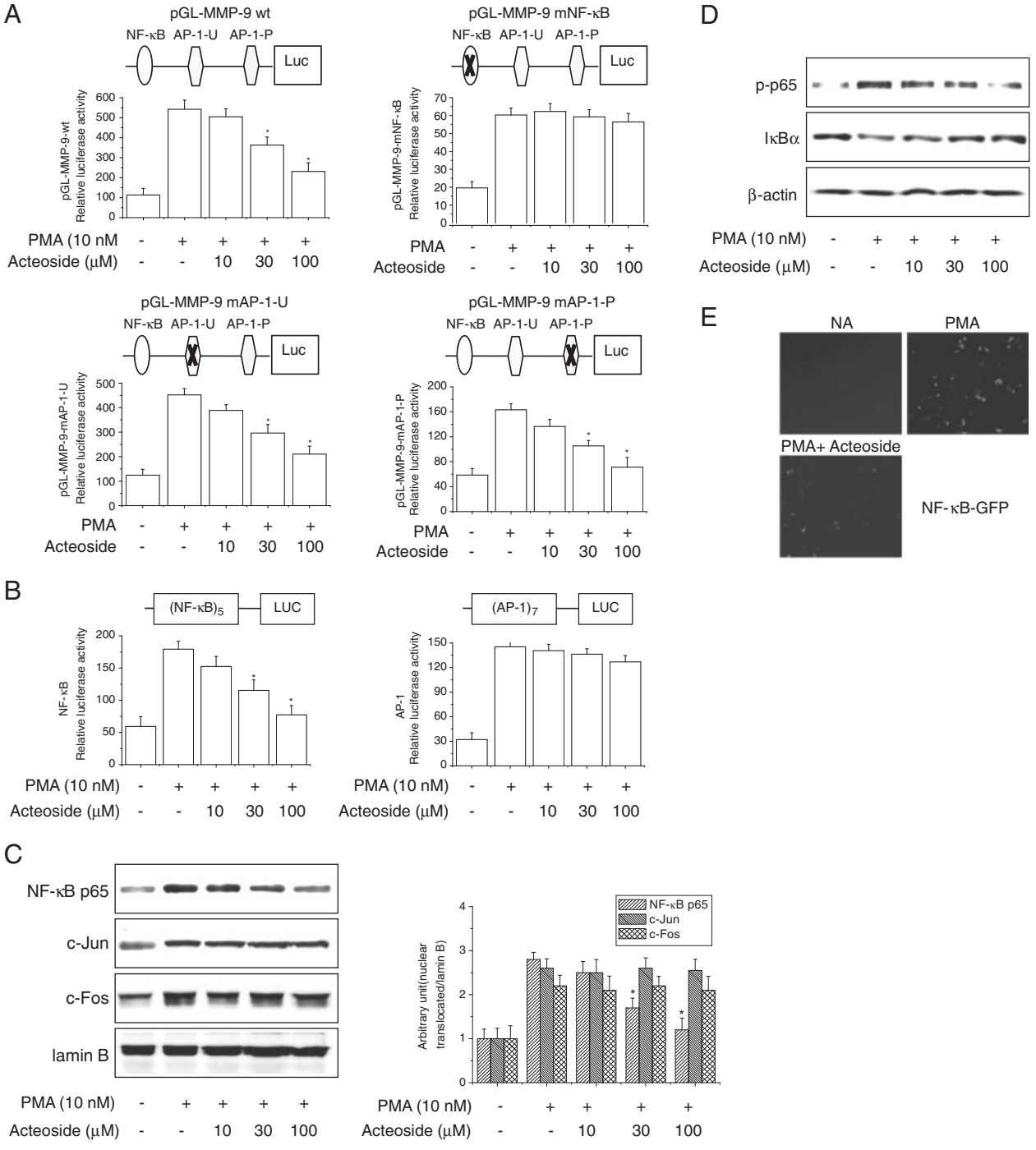

Figure 4. Inhibitory effects of acteoside on PMA-induced NF-κB activation. Mutations were introduced into the NF-κB- or AP-1-binding sites in pGL-MMP-9WT. HT-1080 cells were transfected with pGL-MMP-9WT, pGL-MMP-9mNF-κB, pGL-MMP-9mAP-U, or pGL-MMP-9mAP-P reporter plasmids (A) or with reporter plasmids containing tandem NF-κB- or AP-1-binding sites (B). Cells were cultured with acteoside and/or PMA for 24 h, and the relative luciferase activity level was determined. *Significantly different from PMA treatment alone ($p<0.01$). (C) Effects of acteoside on PMA-induced NF-κB, c-Jun, and c-Fos nuclear translocation. HT-1080 cells were pre-treated with acteoside (10–100 μM) for 1 h, and then treated with PMA (10 nM) for 6 h. The nuclear extracts were subjected to SDS-PAGE, followed by Western blotting with antibodies against NF-κB, c-Jun, c-Fos, and lamin B. *Significantly different from PMA treatment only ($p<0.01$). (D) Effect of acteoside on the PMA-induced IκBα degradation and phosphorylation of p65 and c-Jun. HT-1080 cells were pretreated with acteoside (10–100 μM) for 1 h and treated with 10 nM PMA for 3 h. Whole-cell extracts were subjected to SDS-PAGE, followed by Western blotting with anti-IκBα, anti-phospho-NF-κB p65, and anti-β-actin antibodies. (E) Effects of acteoside on PMA-induced NF-κB activation. Cells were transiently transfected with Lenti-NF-κB-GFP. GFP fluorescence was analyzed by fluorescence microscopy (magnification, × 100).

further determine the promoter structure used by acteoside, we transfected HT-1080 cells with pNF-κB-Luc or pAP-1-Luc plasmids, which contain *luciferase* driven by NF-κB- or AP-1-responsive elements, respectively. As shown in Fig. 4B, acteoside suppressed the NF-κB-responsive promoters in a dose-dependent manner, confirming NF-κB as the target of acteoside. However, acteoside did not suppress the PMA-induced AP-1 activity (Fig. 4B). To investigate which of these transcription factors is involved in the inhibition of *MMP-9* transcription by acteoside, we examined the effect of acteoside on the PMA-stimulated nuclear translocation of p65 (a major subunit of NF-κB) and c-Jun or c-Fos (major subunits of AP-1), which are required for their respective transcriptional activities. Figure 4C shows that the protein levels of NF-κB p65 in the nuclear extracts were dose-dependently decreased following acteoside treatment, whereas no inhibition of the PMA-induced nuclear translocation of c-Jun and c-Fos was observed (Fig. 4C). Furthermore, acteoside inhibited the phosphorylation of NF-κB p65 and degradation of IκBα in a dose-dependent manner (Fig. 4D). To confirm the specificity of the acteoside-mediated inhibitory effects of NF-κB in HT-1080 cells, cells were transiently transfected with reporter vectors that included tandem repeats of the NF-κB-binding sites. As shown in Fig. 4E, treatment with acteoside decreased PMA-mediated GFP fluorescence. Collectively, these data suggest that acteoside regulates the transcriptional activation of *MMP-9* through the inhibition of PMA-stimulated NF-κB activity, but not AP-1 activity.

3.5 Acteoside inhibits MMP-9 activation by suppressing PMA-stimulated NF-κB activity

We further examined whether the activation of NF-κB is involved in PMA-induced MMP-9 expression using a selective NF-κB activation inhibitor, JSH-23 [37]. HT-1080 cells were pretreated with 20 nM JSH-23 for 1 h then stimulated with 10 nM PMA in the presence or absence of 100 μM

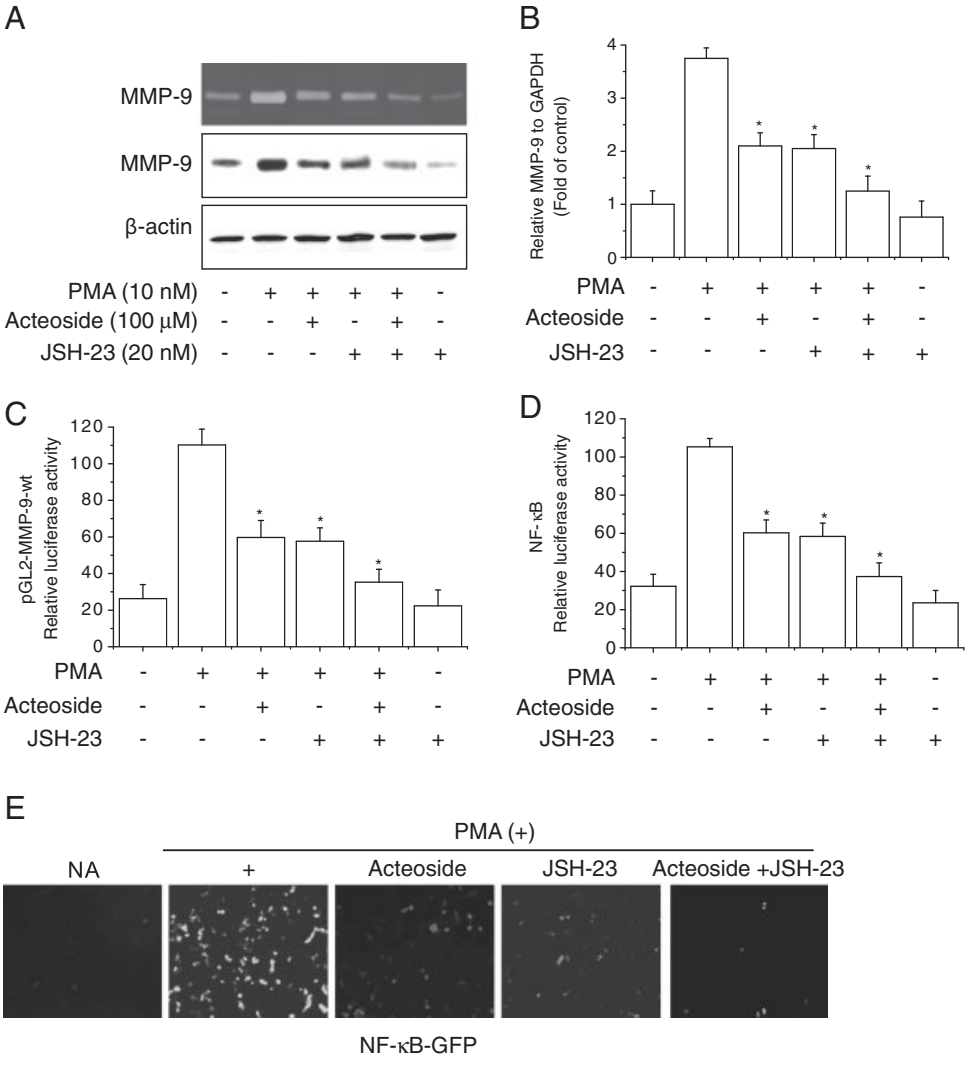

Figure 5. NF-κB is involved in the acteoside-mediated down-regulation of MMP-9. Cells were treated with 10 nM PMA for 24 h in the presence or absence of acteoside or JSH-23. (A) Conditioned media were collected after 24 h and gelatin zymography or Western blotting was performed. (B) *MMP-9* mRNA expression was analyzed by real-time PCR. *GAPDH* expression was included as an internal control. (C and D) HT-1080 cells were transfected with pGL-MMP-9WT and pNF-κB reporter plasmids and cultured with acteoside or JSH-23 and/or PMA for 24 h. Luciferase activity in the cell lysates was determined. *Significantly different from PMA treatment only ($p < 0.01$). (E) Cells were transiently transfected with Lenti-NF-κB-GFP. GFP fluorescence was analyzed by fluorescence microscopy (magnification, × 100).

acteoside for 24 h. The culture media were subjected to gelatin zymography, Western blotting, and real-time PCR. Figure 5A and B indicate that JSH-23 inhibited PMA-induced MMP-9 expression, whereas combined treatment with JSH-23 and acteoside additively reduced PMA-induced MMP-9 expression. To test which of these transcription factors regulates *MMP-9*, cells were transiently transfected with reporter genes that included the wild-type *MMP-9* promoter or a promoter with mutations in the NF-κB site (Fig. 5C–E). As shown in Fig. 5C, JSH-23 inhibited the PMA-induced transcriptional activation of *MMP-9*, and combined treatment with JSH-23 and acteoside additively reduced PMA-induced *MMP-9* transcriptional activation. Furthermore, combined treatment with JSH-23 and acteoside additively reduced PMA-induced NF-κB activity (Fig. 5D and E).

3.6 Acteoside suppresses the PMA-mediated phosphorylation of ERK, JNK, and CaMK

To identify the signal transduction pathways involved in PMA-stimulated MMP-9 expression and its inhibition by acteoside, the effects of specific kinase inhibitors on the

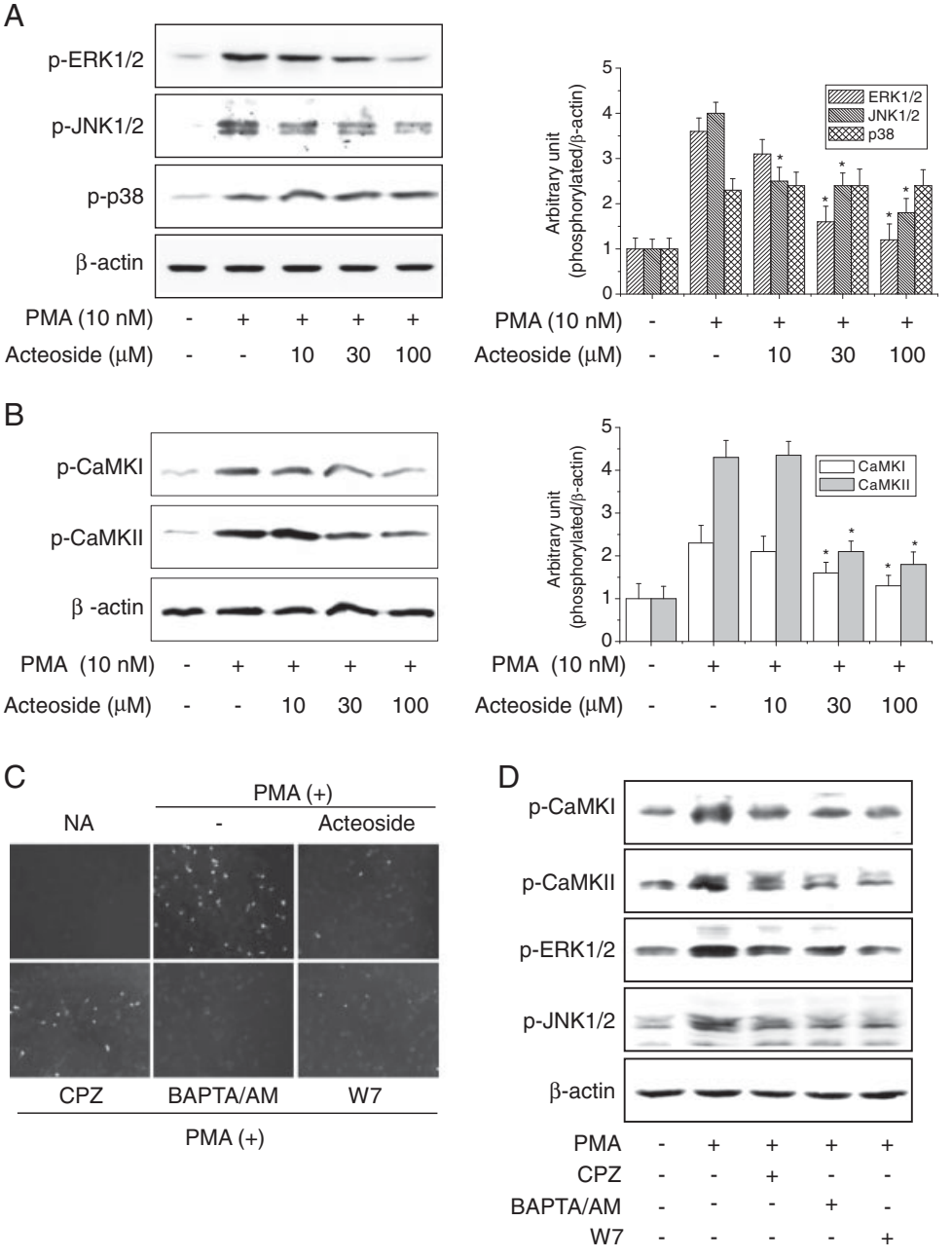

Figure 6. Acteoside inhibits the PMA-induced phosphorylation of CaMKI, CaMKII, ERK1/2, and JNK1/2 in HT-1080 cells. Cells were treated with PMA (10 nM) for 30 min in the presence or absence of acteoside, and the phosphorylation of ERK1/2, JNK1/2, p38 MAPK (A), CaMKI, and CaMKII (B) was measured by Western blotting. β-Actin was included as a loading control. *Significantly different from PMA treatment only ($p<0.01$). (C) Effects of acteoside, BAPTA/AM, W7, or CPZ on the $[Ca^{2+}]_i$ in HT-1080 cells. Cells (2×10^5 cells/mL in a 24-well microtiter plate) were treated with PMA (10 nM) for 30 min in the presence or absence of acteoside, BAPTA/AM, W7, or CPZ for 30 min. The cells were then viewed under a fluorescence microscope (excitation at 385 nm, emission at 512 nm) (magnification, × 100). Each figure is representative of at least three others. (D) Effects of acteoside, BAPTA/AM, W7, or CPZ on the PMA-induced phosphorylation of CaMKI, CaMKII, ERK1/2, and JNK1/2 in HT-1080 cells. Cells were treated with PMA (10 nM) for 30 min in the presence or absence of acteoside (100 μM), BAPTA/AM (10 μM), W7 (40 μM), or CPZ (2 μM), and the phosphorylation of the indicated kinases was measured by Western blotting.

expression of MMP-9 in PMA-induced HT-1080 cells were analyzed by gelatin zymography. PMA-induced MMP-9 secretion was completely inhibited by inhibitors of ERK1/2 (PD98059), p38 MAPK (SB203580), and JNK1/2 (SP600125) (data not shown). To evaluate the effects of acteoside on these signaling cascades, we used antibodies against the phosphorylated activated forms of the kinases and assessed their levels following acteoside treatment. As shown in Fig. 6A, while PMA increased the levels of ERK1/2, JNK1/2, and p38 MAPK phosphorylation, acteoside specifically decreased PMA-induced ERK1/2 and JNK1/2 phosphorylation, whereas the level of phospho-p38 MAPK remained unchanged. These results suggest that acteoside specifically suppresses ERK and JNK activity.

Increased intracellular Ca^{2+} following PMA stimulation [38] is important as both a cofactor for the MAPKs activated by PMA [39] and for the activation of the Ca^{2+}/CaM pathway through binding to CaM [40]. We therefore examined the effects of acteoside on the PMA-induced phosphorylation of CaMKI and CaMKII, which are upstream modulators of MAPK signaling. Figure 6B shows that while PMA activated CaMKI and CaMKII phosphorylation, significant inhibition of this stimulation was observed in the presence of acteoside.

3.7 Acteoside suppresses PMA-induced MMP-9 activation through Ca^{2+}-dependent ERK1/2 and JNK signaling pathways

We investigated the changes in intracellular Ca^{2+} in PMA-treated cells using the fluorescent indicator Fluo-4-AM. PMA was added to HT-1080 cells that had been loaded with 5 μM fluo-4-AM and the cells were viewed by fluorescence microscopy after 30 min (Fig. 6C). We observed a transient increase in Ca^{2+} following PMA treatment (10 nM). As shown in Fig. 6C, pretreatment with acteoside or the intracellular Ca^{2+} chelator BAPTA/AM (5 μM), Ca^{2+}/CaM antagonist W7 (40 μM), or TRPV1 antagonist CPZ (2 μM) blocked the PMA-induced transient increase in Ca^{2+} (Fig. 6C). To evaluate the role of intracellular Ca^{2+} in PMA-mediated signaling, cells were first exposed to BAPTA/AM, W7, or CPZ prior to PMA exposure and analyzed for CaMKI, CaMKII, ERK1/2, and JNK1/2 phosphorylation. As shown in Fig. 6D, BAPTA/AM, W7, and CPZ all modulated CaMKI, CaMKII, ERK1/2, and JNK1/2 phosphorylation.

3.8 Acteoside suppresses invasion and migration *via* Ca^{2+}-dependent NF-κB signaling

As shown in Fig. 7A and B, the level of NF-κB p65 in the nuclear extracts and *NF*-κB promoter activity were decreased by BAPTA/AM, W7, and CPZ treatment (Fig. 7A and B). Furthermore, in the exposed cells, PMA-induced MMP-9 activation was significantly lower than in cells treated with PMA alone (Fig. 7C and D). *In vitro* invasion and migration assays were used to investigate the inhibitory effects of BAPTA/AM, W7, and CPZ on the invasive potency of HT-1080 cells. As shown in Fig. 7E and F, wound-healing and matrigel invasion assays indicated that the migration and invasion of HT-1080 cells were inhibited by an intracellular Ca^{2+} chelator, Ca^{2+}/CaM antagonists, or TRPV1 antagonists. These results suggest that acteoside suppresses PMA-induced invasion and migration and MMP-9 activation *via* Ca^{2+}-dependent CaMK, ERK, and JNK/NF-κB signaling (Fig. 8).

4 Discussion

Accumulating evidence suggests that acteoside, a phenylethanoid glycoside, is a potential anti-cancer agent [7, 10]. However, the effect of acteoside on PMA-induced MMP-9 expression and the invasiveness of HT-1080 fibrosarcoma cells were unclear. Here, we found that acteoside suppressed cell invasion through the inhibition of MMP-9 expression and we examined the detailed molecular mechanisms of this inhibition. Our data support the previous reports regarding the therapeutic potential of acteoside in cancer.

MMPs belong to a family of closely related Ca^{2+}- and zinc-dependent endopeptidases that are involved in the degradation and remodeling of ECM proteins associated with tumorigenic processes [13]. MMPs promote tumor invasion and metastasis, and they regulate host defense mechanisms and normal cell function. Thus, MMP inhibitors are expected to be useful chemotherapeutic agents in the treatment of malignant cancer, osteoarthritis, and rheumatoid arthritis [41, 42].

We first evaluated the inhibitory effects of acteoside on invasion and migration in the absence or presence of PMA in HT-1080 cells. Our data show that acteoside inhibited PMA-induced cell invasion (Fig. 1D). Also, treatment with acteoside only inhibited the cell invasion and migration in a same manner. Our previous study, in which we determined the role of MMPs in PMA-induced invasion, demonstrated that GM6001, a broad-spectrum MMP inhibitor, inhibited the PMA-induced invasion of HT-1080 cells [32], implicating the involvement of MMPs. We therefore sought to determine the effects of acteoside on MMP-9 and -2 expression. In PMA-treated cells, acteoside suppressed the elevated expression and secretion of MMP-9 and -2 (Fig. 1C and 2).

MT1-MMP and TIMPs play a direct or indirect role in pericellular proteolysis and ECM turnover [35]. Therefore, the inhibition of ECM degradation and cell adhesion to ECM molecules could be considered a preventive approach in cancer metastasis. We thus determine the effects of acteoside on MT1-MMP, TIMP-1, and -2 expression. Our results show that acteoside significantly reduced MT1-MMP levels (Fig. 3). However, TIMP-1 and -2 expression was unchanged by acteoside in our system, possibly due to system- and

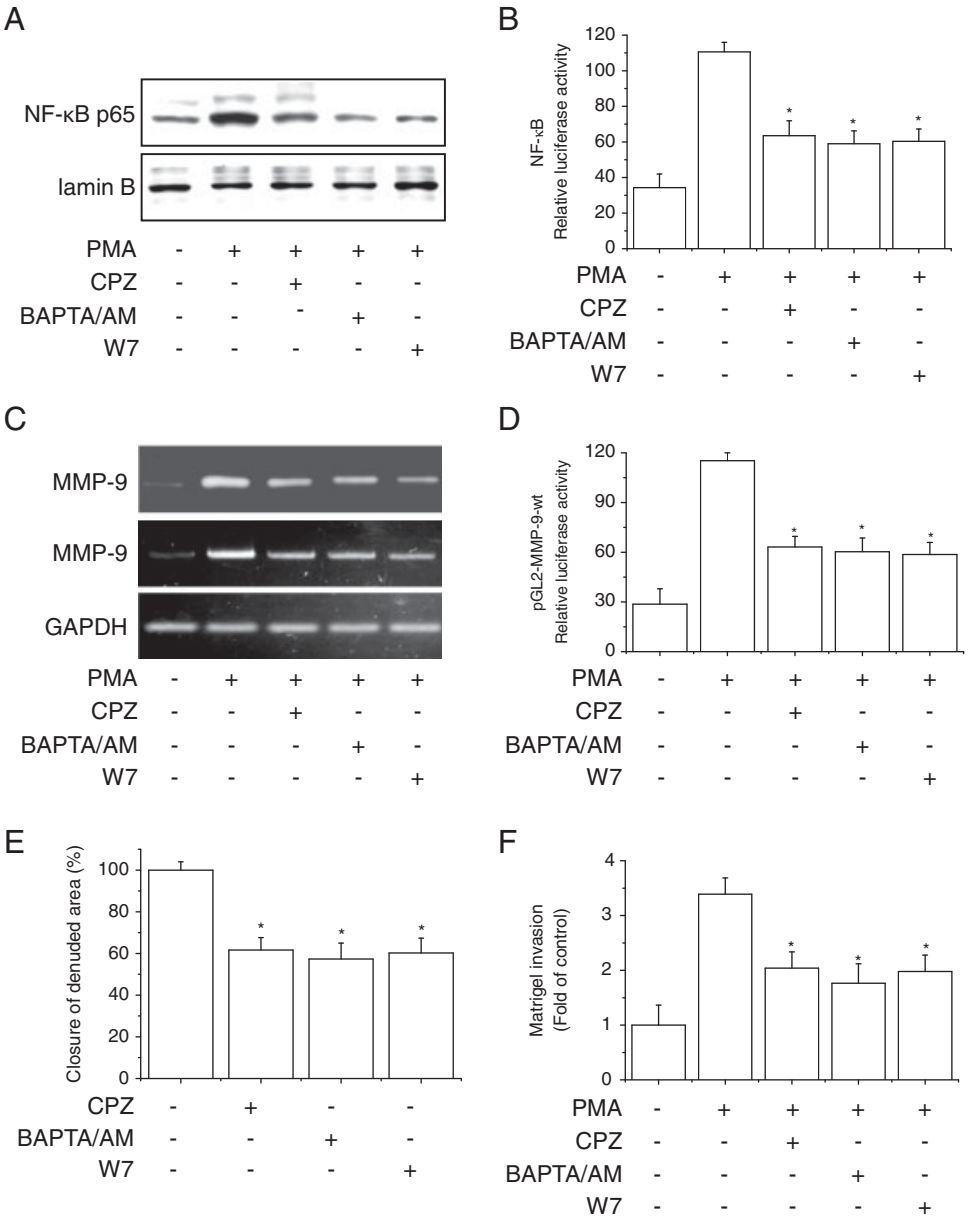

Figure 7. Effect of BAPTA/AM, W7, or CPZ on PMA-induced NF-κB p65 translocation in HT-1080 cells. (A) Cells were pretreated with BAPTA/AM (10 μM), W7 (40 μM), or CPZ (2 μM) for 1 h followed by treatment with 10 nM PMA for 6 h. Nuclear extracts were subjected to SDS-PAGE followed by Western blotting with anti-NF-κB p65 and -lamin B antibodies. (B) Cells were transfected with pNF-κB reporter plasmids and cultured with BAPTA/AM (10 μM), W7 (40 μM), CPZ (2 μM), and/or PMA for 24 h. Luciferase activity in the cell lysates was determined. *Significantly different from PMA treatment only ($p<0.01$). (C) Effects of BAPTA/AM, W7, or CPZ on PMA-induced MMP-9 activity in HT-1080 cells. Cells were pretreated with the compounds for 1 h followed by treatment with 10 nM PMA for 24 h. MMP-9 activity in the medium was assessed by gelatin zymography and Western blotting. (D) Cells were transfected with pGL-MMP-9WT reporter plasmids. Luciferase activity in the cell lysates was determined. The data are expressed as the mean ± SD of triplicate experiments. *Significantly different from PMA treatment only ($p<0.01$). (E and F) Effects of BAPTA/AM, W7, or CPZ on the migration and invasion of HT-1080 cells. (E) Cells were scratched with a pipette tip and then treated with BAPTA/AM (10 μM), W7 (40 μM), or CPZ (2 μM) for 24 h. Migrating cells were imaged by phase-contrast microscopy. The data are expressed as the mean ± SD of triplicate experiments. *Significantly different from the control ($p<0.01$). (F) Cells were pretreated with BAPTA/AM (10 μM), W7 (40 μM), or CPZ (2 μM) followed by PMA treatment (10 nM) for 24 h. The cells on the bottom of the filter were then counted. The data are expressed as the mean ± SD of triplicate experiments. *Significantly different from PMA treatment only ($p<0.01$).

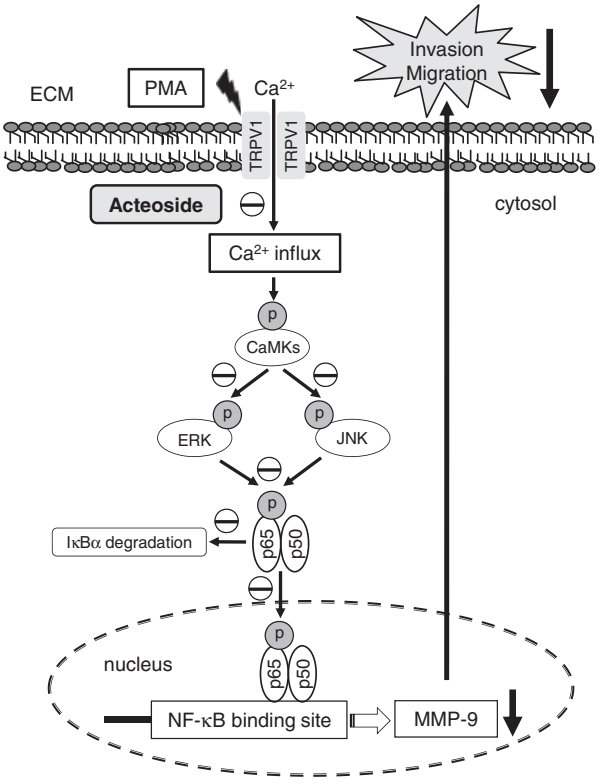

Figure 8. Model of the inhibitory effects of acteoside on PMA-induced migration and invasion. Schematic highlights of the signaling steps identified in this study. Acteoside significantly suppressed MMP-9 activation by blocking the influx of Ca^{2+} and subsequent CaMK/ERK and JNK/NF-κB signaling. This inhibition resulted in reduced migration and invasion of human fibrosarcoma cells. O minus, inhibition, or blockade; p, phosphorylation.

concentration-specific effects (Fig. 3). These results suggest that acteoside decreases pro-MMP-2 activation by reducing MT1-MMP levels.

We further investigated the mechanisms of *MMP-9* transcriptional regulation by acteoside. The *MMP-9* promoter contains *cis*-acting regulatory elements for transcription factors, including two AP-1 sites and an NF-κB site [32]. Acteoside suppressed MMP-9 induction by repressing transcriptional activation of the *MMP-9* promoter (Fig. 4A). Mutational analysis of the promoter revealed that the major target of acteoside was the NF-κB sites, a finding that was confirmed using reporter plasmids containing synthetic elements specific for these transcription factors (Fig. 4A and B). In this study, acteoside did not block the increased reporter activity of the AP-1 promoter in the lysates obtained from the cells treated with PMA. This suggests that the blocking effect of MMP-9 induction by acteoside may not be associated with the AP-1 activation pathway. Several lines of evidence have shown a close relationship between NF-κB or AP-1 activation and enhanced MMP-9 expression in various cell types. Acteoside has been demonstrated to exhibit various anti-carcinogenic mechanisms. Pastor *et al.* [5] reported that acteoside impaired NF-κB and AP-1 DNA binding activity in HaCaT cells. Furthermore, Lee *et al.* [43] reported that acteoside blocks lipopolysaccharide-induced inducible nitric oxide synthase expression in mouse macrophage RAW264.7 cells. As the expression of inducible nitric oxide synthase is dependent on NF-κB and AP-1 activation, our evidence that acteoside did not inhibit the promoter activity of AP-1 in HT-1080 cells suggests that acteoside may have some cell type specificity. Additionally, acteoside blocked the translocation of NF-κB p65 to the nucleus in PMA-treated cells; however, suppression of the PMA-induced translocation of c-Fos and c-Jun (components of AP-1) was not observed (Fig. 4C). Acteoside also inhibited the phosphorylation of NF-κB p65 and the degradation of IκBα (Fig. 4D). We also assessed the transcriptional activity of NF-κB and AP-1 and found that acteoside decreased PMA-mediated NF-κB-GFP reporter fluorescence (Fig. 4D). We next investigated the functional significance of NF-κB transactivation in MMP-9 activation. Treatment with JSH-23, a potent inhibitor of NF-κB transcriptional activation, reduced the PMA-induced enzymatic activity and expression of MMP-9 (Fig. 5A–C). JSH-23 also reduced the PMA-induced transcriptional activity of NF-κB (Fig. 5D and E). These findings collectively suggest that acteoside inhibits the PMA-induced activation of MMP-9 by suppressing NF-κB activation in HT-1080 cells.

Several reports have shown that Ca^{2+} channel antagonists have anti-cancer effects by inducing cytotoxicity and apoptosis in human colon cancer, breast cancer, and lung cancer cells [44, 45]. It has been shown that verapamil reverses the resistance of cancer cells to some chemotherapeutic agents [46]. Interestingly, recent studies have demonstrated that acteoside inhibited the IgE-mediated Ca^{2+} influx in RBL-2H3 cells [30]. Acteoside also inhibited the glutamate-induced Ca^{2+} influx in rat cortical cells [31].

Previous studies indicated that TRPV1 induces Ca^{2+} influx and TRPV1 can be activated by tissue injury or inflammation and is also modulated by numerous mediators, including growth factors, neurotransmitters, chemokines, cytokines, and PMA [38, 47]. Alterations in Ca^{2+} are important for the function of several cell-signaling pathways; for example, Ca^{2+} can stimulate MAPK signaling *via* Ca^{2+}/CaM-dependent CaMKs, a pathway involved in cell migration [48]. We identified the signaling pathway-mediated regulation of *MMP-9* in PMA-induced cells in response to acteoside treatment. Acteoside suppressed the PMA-induced phosphorylation of CaMKI, CaMKII, ERK1/2, and JNK1/2, which are involved in PMA-induced cell invasion through MMP-9 expression (Fig. 6A and B). Acteoside also inhibited the PMA-induced Ca^{2+} influx in HT-1080 cells (Fig. 6C). Furthermore, BAPTA/AM (intracellular Ca^{2+} chelator), W7 (Ca^{2+}/CaM antagonist), and CPZ (TRPV1 antagonist) inhibited the PMA-induced phos-

phorylation of CaMKI, CaMKII, ERK1/2, and JNK. In addition, BAPTA/AM, W7, and CPZ also inhibited the activation of NF-κB (Fig. 7A and B), as well as PMA-induced MMP-9 expression (Fig. 7C and D), cell invasion, and migration (Fig. 7E and F).

In summary, the present data demonstrate that acteoside inhibits the PMA-induced invasion and migration of human fibrosarcoma cells *via* Ca^{2+}-dependent CaMK, ERK, and JNK/NF-κB signaling. Acteoside therefore has potential as a potent anti-cancer drug in the treatment of fibrosarcoma metastasis.

This study was supported by a grant of the Korea Healthcare technology R&D Project, Ministry for Health, Welfare & Family Affairs, Republic of Korea (A084869).

The authors have declared no conflict of interest.

5 References

[1] Sporn, M. B., Suh, N., Chemoprevention of cancer. *Carcinogenesis* 2000, *21*, 525–530.

[2] Wong, I. Y., He, Z. D., Huang, Y., Chen, Z. Y., Antioxidative activities of phenylethanoid glycosides from *Ligustrum purpurascens*. *J. Agric. Food Chem.* 2001, *49*, 3113–3319.

[3] Shindo, K., Saito, E., Sekiya, M., Matsui, T., Koike, Y., Antioxidative activity of the flower of *Torenia fournieri*. *J. Nat. Med.* 2008, *62*, 247–248.

[4] Chiou, W., Lin, L., Chen, C., Acteoside protects endothelial cells against free radical-induced oxidative stress. *J. Pharm. Pharmacol.* 2004, *56*, 743–748.

[5] Pastore, S., Potapovich, A., Kostyuk, V., Mariani, V. *et al.*, Plant polyphenols effectively protect HaCaT cells from ultraviolet C-triggered necrosis and suppress inflammatory chemokine expression. *Ann. NY Acad. Sci.* 2009, *1171*, 305–313.

[6] Sheng, G. Q., Zhang, J. R., Pu, X. P., Ma, J. *et al.*, Protective effect of verbascoside on 1-methyl-4-phenylpyridinium ion-induced neurotoxicity in PC12 cells. *Eur. J. Pharmacol.* 2002, *451*, 119–124.

[7] Ohno, T., Inoue, M., Ogihara, Y., Saracoglu, I., Antimetastatic activity of acteoside, a phenylethanoid glycoside. *Biol. Pharm. Bull.* 2002, *25*, 666–668.

[8] Nagao, T., Abe, F., Okabe, H., Antiproliferative constituents in the plants 7. Leaves of *Clerodendron bungei* and leaves and bark of *C. trichotomum*. *Biol. Pharm. Bull.* 2001, *24*, 1338–1341.

[9] Inoue, M., Sakuma, Z., Ogihara, Y., Sarcoglu, I., Induction of apoptotic cell death in HL-60 cells by acteoside, a phenylpropanoid glycoside. *Biol. Pharm. Bull.* 1998, *21*, 81–83.

[10] Wartenberg, M., Budde, P., De Mareés, M., Grünheck, F. *et al.*, Inhibition of tumor-induced angiogenesis and matrix-metalloproteinase expression in confrontation cultures of embryoid bodies and tumor spheroids by plant ingredients used in traditional Chinese medicine. *Lab. Invest.* 2003, *83*, 87–98.

[11] Kajanne, R., Miettinen, P., Mehlem, A., Leivonen, S. K. *et al.*, EGF-R regulates MMP function in fibroblasts through MAPK and AP-1 pathways. *J. Cell. Physiol.* 2007, *212*, 489–497.

[12] John, A., Tuszynski, G., The role of matrix metalloproteinases in tumor angiogenesis and tumor metastasis. *Pathol. Oncol. Res.* 2001, *7*, 14–23.

[13] Sato, H., Takino, T., Okada, Y., Cao, J. *et al.*, A matrix metalloproteinase expressed on the surface of invasive tumour cells. *Nature* 1994, *370*, 61–65.

[14] Gossas, T., Danielson, U. H., Characterization of Ca^{2+} interactions with matrix metallopeptidase-12: implications for matrix metallopeptidase regulation. *Biochem. J.* 2006, *398*, 393–398.

[15] Mukhopadhyay, S., Munshi, H. G., Kambhampati, S., Sassano, A. *et al.*, Calcium-induced matrix metalloproteinase 9 gene expression is differentially regulated by ERK1/2 and p38 MAPK in oral keratinocytes and oral squamous cell carcinoma. *J. Biol. Chem.* 2004, *279*, 33139–33146.

[16] Kohn, E. C., Jacobs, W., Kim, Y. S., Alessandro, R. *et al.*, Calcium influx modulates expression of matrix metalloproteinase-2 (72-kDa type IV collagenase, gelatinase A). *J. Biol. Chem.* 1994, *269*, 21505–21511.

[17] Sudbeck, B. D., Pilcher, B. K., Pentland, A. P., Parks, W. C., Modulation of intracellular calcium levels inhibits secretion of collagenase 1 by migrating keratinocytes. *Mol. Biol. Cell* 1997, *8*, 811–824.

[18] Pedersen, S. F., Owsianik, G. B., Nilius, B., TRP channels: an overview. *Cell Calcium* 2005, *38*, 233–352.

[19] Bevan, S., Hothi, S., Hughes, G., James, I. F. *et al.*, Capsazepine: a competitive antagonist of the sensory neurone excitant capsaicin. *Br. J. Pharmacol.* 1992, *107*, 544–552.

[20] Ramer, R., Merkord, J., Rohde, H., Hinz, B., Cannabidiol inhibits cancer cell invasion via upregulation of tissue inhibitor of matrix metalloproteinases-1. *Biochem. Pharmacol.* 2010, *79*, 955–966.

[21] Rathee, P. K., Distler, C., Obreja, O., Neuhuber, W. *et al.*, PKA/AKAP/VR-1 module: a common link of Gs-mediated signaling to thermal hyperalgesia. *J. Neurosci.* 2002, *22*, 4740–4745.

[22] Dai, Y., Moriyama, T., Higashi, T., Togashi, K. *et al.*, Proteinase-activated receptor 2-mediated potentiation of transient receptor potential vanilloid subfamily 1 activity reveals a mechanism for proteinase-induced inflammatory pain. *J. Neurosci.* 2004, *24*, 4293–4299.

[23] Wu, Z. Z., Chen, S. R., Pan, H. L., Transient receptor potential vanilloid type 1 activation down-regulates voltage-gated calcium channels through calcium-dependent calcineurin in sensory neurons. *J. Biol. Chem.* 2005, *280*, 18142–18151.

[24] Mercure, M. Z., Ginnan, R., Singer, H. A., CaM kinase II delta2-dependent regulation of vascular smooth muscle cell polarization and migration. *Am. J. Physiol. Cell. Physiol.* 2008, *294*, C1465–C1475.

[25] Colbran, R. J., Soderling, T. R., Calcium/calmodulin-dependent protein kinase II. *Curr. Top. Cell. Regul.* 1990, *31*, 181–221.

[26] Catterall, W. A., Structure and regulation of voltage-gated Ca^{2+} channels. *Annu. Rev. Cell. Dev. Biol.* 2000, *16*, 521–555.

[27] Wei, J. W., Morris, H. P., Hickie, R. A., Positive correlation between calmodulin content and hepatoma growth rates. *Cancer Res.* 1982, *42*, 571–574.

[28] Shim, J. S., Lee, J., Kim, K. N., Kwon, H. J., Development of a new Ca^{2+}/calmodulin antagonist and its anti-proliferative activity against colorectal cancer cells. *Biochem. Biophys. Res. Commun.* 2007, *359*, 747–751.

[29] Roderick, H. L., Cook, S. J., Ca^{2+} signalling checkpoints in cancer: remodelling Ca^{2+} for cancer cell proliferation and survival. *Nat. Rev. Cancer* 2008, *8*, 361–375.

[30] Lee, J. H., Lee, J. Y., Kang, H. S., Jeong, C. H. *et al.*, The effect of acteoside on histamine release and arachidonic acid release in RBL-2H3 mast cells. *Arch. Pharm. Res.* 2006, *29*, 508–513.

[31] Koo, K. A., Kim, S. H., Oh, T. H., Kim, Y. C., Acteoside and its aglycones protect primary cultures of rat cortical cells from glutamate-induced excitotoxicity. *Life Sci.* 2006, *79*, 709–716.

[32] Eberhardt, W., Schulze, M., Engels, C., Klasmeier, E. *et al.*, Glucocorticoid-mediated suppression of cytokine-induced matrix metalloproteinase-9 expression in rat mesangial cells: involvement of nuclear factor-kappaB and Ets transcription factors. *Mol. Endocrinol.* 2002, *16*, 1752–1766.

[33] Johnson, M. R., Wang, K., Smith, J. B., Heslin, M. J. *et al.*, Quantitation of dihydropyrimidine dehydrogenase expression by real-time reverse transcription polymerase chain reaction. *Anal. Biochem.* 2000, *278*, 175–184.

[34] Hwang, Y. P., Yun, H. J., Kim, H. G., Han, E. H. *et al.*, Suppression of PMA-induced tumor cell invasion by dihydroartemisinin via inhibition of PKCalpha/Raf/MAPKs and NF-kappaB/AP-1-dependent mechanisms. *Biochem. Pharmacol.* 2010, *79*, 1714–1726.

[35] Egeblad, M., Werb, Z., New functions for the matrix metalloproteinases in cancer progression. *Nat. Rev. Cancer* 2002, *2*, 161–174.

[36] Kazes, I., Elalamy, I., Sraer, J. D., Hatmi, M. *et al.*, Platelet release of trimolecular complex components MT1-MMP/TIMP2/MMP2: involvement in MMP2 activation and platelet aggregation. *Blood* 2000, *96*, 3064–3069.

[37] Shin, H. M, Kim, M. H., Kim, B. H., Jung, S. H. *et al.*, Inhibitory action of novel aromatic diamine compound on lipopolysaccharide-induced nuclear translocation of NF-kappaB without affecting IkappaB degradation. *FEBS Lett.* 2004, *571*, 50–54.

[38] Buys, S. S., Keogh, E. A., Kaplan, J., Fusion of intracellular membrane pools with cell surfaces of macrophages stimulated by phorbol esters and calcium ionophores. *Cell* 1984, *38*, 569–576.

[39] Cox, M. E., Parsons, S. J., Roles for protein kinase C and mitogen-activated protein kinase in nicotine-induced secretion from bovine adrenal chromaffin cells. *J. Neurochem.* 1997, *69*, 1119–1130.

[40] Soderling, T. R., The Ca-calmodulin-dependent protein kinase cascade. *Trends Biochem. Sci.* 1999, *24*, 232–236.

[41] Lia, N. G., Shib, Z. H., Tang, Y. P., Duan, J. A., Selective matrix metalloproteinase inhibitors for cancer. *Curr. Med. Chem.* 2009, *16*, 3805–3827.

[42] Li, X., Wu, J. F., Recent developments in patent anti-cancer agents targeting the matrix metalloproteinases (MMPs). *Recent Pat. Anticancer Drug Discov.* 2010, *5*, 109–141.

[43] Lee, J. Y., Woo, E. R., Kang, K. W., Inhibition of lipopolysaccharide-inducible nitric oxide synthase expression by acteoside through blocking of AP-1 activation. *J. Ethnopharmacol.* 2005, *97*, 561–566.

[44] Wondergem, R., Bartley, J. W., Menthol increases human glioblastoma intracellular Ca2+, BK channel activity and cell migration. *J. Biomed. Sci.* 2009, *16*, 90–97.

[45] Zhang, C., Lv, F., Zhou, L., Li, X. *et al.*, Effect of verapamil on the expression of EGFR and NM23 in A549 human lung cancer cells. *Anticancer Res.* 2009, *29*, 27–32.

[46] Mayur, Y. C., Jagadeesh, S., Thimmaiah, K. N., Targeting calmodulin in reversing multidrug resistance in cancer cells. *Mini Rev. Med. Chem.* 2006, *12*, 1383–1389.

[47] Ma, W., Quirion, R., Inflammatory mediators modulating the transient receptor potential vanilloid 1 receptor: therapeutic targets to treat inflammatory and neuropathic pain. *Expert Opin. Ther. Targets* 2007, *11*, 307–320.

[48] He, Y. Y., Huang, J. L., Chignell, C., Delayed and sustained activation of extracellular signal-regulated kinase in human keratinocytes by UVA. *J. Biol. Chem.* 2004, *279*, 53867–53874.

